JOURNAL OF ENVIRONMENTAL SCIENCES 71 (2018) 136–149

Available online at www.sciencedirect.com

ScienceDirect

www.elsevier.com/locate/jes

JES JOURNAL OF ENVIRONMENTAL SCIENCES

www.jesc.ac.cn

Characteristics of the pollutant emissions in a tunnel of Shanghai on a weekday

Rui Li[1], *Ya Meng*[1], *Hongbo Fu*[1,2,3,*], *Liwu Zhang*[1], *Xingnan Ye*[1], *Jianmin Chen*[1,*]

1. *Shanghai Key Laboratory of Atmospheric Particle Pollution and Prevention, Department of Environmental Science & Engineering, Institute of Atmospheric Sciences, Fudan University, Shanghai, 200433, P.R. China*
2. *Shanghai Institute of Pollution Control and Ecological Security, Shanghai 200092, P.R. China*
3. *Collaborative Innovation Center of Atmospheric Environment and Equipment Technology (CICAEET), Nanjing University of Information Science and Technology, Nanjing 210044, China*

ARTICLE INFO

Article history:
Received 18 September 2017
Revised 11 November 2017
Accepted 14 November 2017
Available online 23 November 2017

Keywords:
Tunnel
Vehicle emission
Size distribution
Morphology

ABSTRACT

Tunnel displays a typical semi-closed environment, and multitudes of the pollutants tend to accumulate. The samples of gaseous pollutants and particulate matter (PM) were collected from the Xiangyin tunnel at Shanghai to investigate the characteristics of the pollutant emissions. The results indicated that both gaseous pollutants and PM exhibited much higher concentrations during the rush hours in the morning and at night due to vehicle emission. Two peaks of the PM concentration were observed in the scope of 0.7-1.1 and 3.3–4.7 μm, accounting for 14.6% and 20.3% of the total concentrations, respectively. Organic matter (OM), EC, and many water-soluble ions were markedly higher at the rush hours in the morning than those at night, implicating comprehensive effects of vehicle types and traffic volume. The particle number concentrations exhibited two peaks at Aitken mode (25 nm and 100 nm) and accumulation mode (600 nm), while the particle volume concentration displayed high values at the accumulation mode (100–500 nm) and coarse mode (2.5–4.0 μm). The peak around 100 nm was detected in the morning rush hours, but it diminished with the decrease of the traffic volume. Individual-particle analysis revealed that main particles in the tunnel were Fe-rich particles, K-rich particles, mineral particles, Ca–S rich particles and Al–Si particles. The particles collected at the rush hours displayed marked different morphologies, element concentrations and particle sizes compared to the ones collected at the non-rush period. The data presented herein could shed a light on the feature of vehicle emissions.

Introduction

Aerosol particles play significant roles on climate by changing the energy transfer through the radiative forcing, and potentially cause adverse health effects as carriers of toxic chemicals (Li et al., 2008; Lin et al., 2005; Jacobson, 2001). Some aerosol particles probably absorb or scatter the solar radiation, thereby influencing the global climate (Anenberg et al., 2012; Liu et al., 2014). Health studies have proved that fine particulate ($PM_{2.5}$) showed close relationship to respiratory and cardiovascular disease, and even increased risk for cancer or death (Adar et al., 2007; Liu et al., 2015). Exposure to organic

* *Corresponding authors. E-mail addresses:* fuhb@fudan.edu.cn (H. Fu), jmchen@fudan.edu.cn (J. Chen).

https://doi.org/10.1016/j.jes.2017.11.015
1001-0742 © 2017 The Research Center for Eco-Environmental Sciences, Chinese Academy of Sciences. Published by Elsevier B.V.

particles was associated with allergies and adverse respiratory effects, frequently expressed as asthma or chronic obstructive pulmonary disease (Lerner et al., 2012).

Vehicle emissions have been considered as a main source of atmospheric pollutants (Chiang and Huang, 2009). About 23% of NO_x, 17% of CO, and more than 50% of volatile organic compounds (VOCs) were released from vehicle emissions in East China (Fu et al., 2013; Chiang et al., 2007; Lee et al., 2002). Moreover, about 6.7 million tons and 8.3 million tons of $PM_{2.5}$ and PM_{10} were emitted by vehicles in Pearl River Delta in 2006, respectively (Cui et al., 2016). The occurrence of hazy days has been increasing since 2005, particularly in some megacities of China (Tong et al., 2007). Some gaseous pollutants (*e.g.*, NO_x and VOCs) were the key precursors of second species, such as ozone, in ambient air, which probably induced a severe fog-haze episode (Zhou et al., 2014). S. Guo et al. (2014), L. Guo et al. (2014) concluded that photochemical oxidation of NO_x and SO_2 emitted from traffic emissions was primarily responsible for urban haze in China. Hu et al. (2015) also reported that $Zn(NO_3)_2$ and $ZnSO_4$ displayed higher concentrations in the haze-fog episodes compared with the clear episodes. The number fractions of organic carbon principally derived from vehicle emissions reached to 30% in Shanghai (Hu et al., 2016). In recent years, the numbers of automobiles increased from 187 to 296 million between 2011 and 2015 in China, seriously deteriorating air quality (Cai et al., 2010). Thus, to address the feature of vehicle exhausts has become a crucial issue to understand the influence of vehicle emissions on air quality in China.

It is an arduous challenge to investigate the characteristics of vehicle emissions accurately to ambient air because these pollutants emitted from vehicles are inclined to mix with PM rapidly in the atmosphere. To date, many methods have been used to address vehicle emission features, including the engine dynamometer test (Na et al., 2015), remote sensing (Andrew, et al., 2003), and tunnel research (Liu et al., 2012). Dynamometer test is costly and its procedure is complex. Furthermore, the test condition of the dynamometer cannot absolutely simulate the realistic driving state. Remote sensing just measures emissions of individual vehicle as they drive by a roadside sensor, but not obtain fleet-average emission results. Moreover, the dynamometer test and remote sensing cannot distinguish the vehicle emissions from other sources effectively. In contrast, tunnel research not only reflects the real driving environment with less environmental interference, but also makes use of the fact that emissions from vehicles inside tunnels could be isolated from other sources easily. Additionally, there is an increased emissions in concentration and prolonged exposure to the pollutants emitted by the vehicles due to the confined space and inadequate ventilation (El-Fadel and Hashisho, 2001; Brito et al., 2013; Ho et al., 2004). Thus, the research on the tunnel has become a popular mean to study the characteristics of vehicle emissions.

A growing body of tunnel studies has been conducted in megacities on the world. Many tunnel studies focused on the characteristics of emissions including concentrations, components and emission factors of the pollutants. Ma et al. (2011) reported that the concentrations of CO, SO_2, and NO_x, reached to 12–39 ppm, 20–48 ppb, and 1.2–3.1 ppm, respectively, in the Hsueh-shan tunnel. Ho et al. (2009) reported that the VOC concentrations in Shing Mun tunnel were about 5–10 times higher than those in the ambient air of Hong Kong. It were generally considered that benzene, toluene, xylene and isoprene were the major species of VOCs, all of which generally exhibit higher concentrations in the tunnel due to high intensity emission of vehicle exhausts (Chiang et al., 2007). Carbonaceous compounds and water-soluble ions were primary components of PM collected from the tunnel (Pio et al., 2013). However, the components and concentrations of the pollutants varied significantly in the different tunnels probably due to the impacts of engine type, fuel consumption, vehicle characteristics and other uncertain factors (Alves et al., 2015). It was well documented that the number, speed, age, and type of vehicle showed remarkable effects on the concentrations and species of gaseous pollutants and atmospheric PM inside the tunnel (Schmid et al., 1997). Vehicle number generally showed a significantly positive relevance with the pollutant concentration inside the tunnel (Zhou et al., 2014). Especially, the emission factors in the Wuzushan tunnel were higher than those in the Kuixinglou tunnel as the result of high proportion of diesel vehicle in the former (Cui et al., 2016). The NO_x emission increased with vehicle speed for uphill driving and possessed higher values for uphill driving than those for downhill driving (Andrew et al., 2003). However, few studies concerned about the morphology and mixing state of PM within the tunnel, which were also sensitive to the vehicle emissions. Knowledge of the morphology and mixing state of individual particles in the tunnel was crucial to understand the vehicle emission features (Li et al., 2016).

In the present study, the PM samples were collected and gaseous pollutants were on-line analyzed over a 24-hr period in the Xiangyin tunnel of Shanghai. The main objectives of this study are: (1) to investigate the diurnal variation of gaseous pollutants and PM inside the tunnel, (2) to determine the concentration and composition of PM, and (3) to decipher the number and volume concentrations, size distribution and morphology of PM at a single-particle level.

1. Experimental section

The samples were collected in the Xiangyin tunnel, which was located at the middle ring of Shanghai. This tunnel is a length of 2.6 km with the maximum speed limit of 80 km/hr. Diesel and gasoline vehicles were main vehicle types across the Xiangyin tunnel. The proportion of diesel vehicles through Xiangyin tunnel was high in the daytime, while they were relatively low at night because diesel vehicles were prohibited entering downtown area since the evening rush hours. The samples including aerosol particles and gaseous pollutants inside the tunnel were collected at the midpoint of the tunnel, and the ambient samples outside the tunnel were collected in the site about 50 m far from the exit of the tunnel. Ambient air samples in the tunnel were collected once each hour from 14:30 on April 24th to 14:30 on April 25th, 2013. The sampling period was a weekday, which could represent the pollution status in the tunnel in the weekdays. Ambient air was collected at a flow rate of 1 L/min. The samples were analyzed within one day after the sampling.

Particles inside the tunnel were collected in the eight size fractions: 0.4–0.7, 0,7–1.1, 1.1–2.1, 2.1–3.3, 3.3–4.7, 4.7–5.8, 5.8–9,

and >9 μm, respectively. The sampling pump flow rate was set at 28.3 L/min. Before the sampling, the quartz filters were pre-heated at 550°C for 6 hr and were then equilibrated at 22°C and 40% ± 5% relative humidity (RH) for 24 hr, and then weighed. After the sampling, the filters were reconditioned and stored in a freezer at –4°C until analysis. The Teflon filters were balanced at RH (40% ± 5%) and 20°C for 24 hr.

A wide-range particle spectrometer (WPSTM, MSP, USA) was applied to determine the size distribution of aerosol particles in the range of 10–1000 nm. The sampling pump flow rate was set at 1.0 L/min. WPS was a high-resolution aerosol spectrometer, which combined the principles of the differential mobility analysis (DMA), the laser light scattering (LPS), and condensation particle counting (CPC). Particles with the diameter over 500 nm and those with the diameter of 10–500 nm were analyzed by LPS channel and DMA + CPC channel, respectively. The number, surface concentrations, volume concentrations, and size distributions of the particles could be achieved by WPS after a parameter correction.

For transmission electron microscopy (TEM) analysis, individual particles were sampled directly on the 300-mesh copper grids coupled with carbon films using an individual-stage cascade impactor. The sampling periods depended on the particle concentration, ranging from 30 sec to 300 sec. The samples were preserved in the plastic carriers in order to reduce the exposure to the air. More information about sampling process were previously described by S. Guo et al. (2014), L. Guo et al. (2014).

1.1. Chemical analysis

1.1.1. Gaseous pollutants analysis

The measurements of SO_2, and NO/NO_2 were performed using SO_2 analyzer (Model 42i, Thermo scientific) and NO_x analyzer (Model 42i, Thermo scientific), respectively. The detection limit of SO_2 and NO/NO_2 were 1.0 and 0.4 ppb, respectively. The CO concentration was determined through nondispersive infrared analyzer (Model 300; Teledyne Advanced Pollution Instrumentation, USA), which showed a detection limit of 30 ppb. The concentrations of VOC were determined using an Entech 7100A pre-concentrator (Entech Inc., USA) followed by a GC–MS system (Finnigan Trace GC/Trace DSQ). The method detection limit (MDL) for analyzed VOCs were 0.50 $\mu g/m^3$. The relative standard deviations on average for all of the compounds were less than 10% and the recovery of the reference materials was 90%–110%. The VOC measurements were described previously in detail by Mao et al. (2009).

1.1.2. Ion analysis

Each sample was extracted ultrasonically for 20 min using 5 mL of ultra-pure water. Filtrates were stored in a clean tube at 4°C for analysis after passing through the microporous membranes. The concentrations of inorganic ions (SO_4^{2-}, NO_3^-, NH_4^+, Cl^-, K^+, Ca^{2+}, Na^+, and Mg^{2+}) were determined using ion chromatography (IC, Dionex ICS 2000, USA). Weak base (76.2 mM NaOH + H_2O) and weak acid (20 mM MSA) were utilized as anion detection and cation detection, respectively. The relative standard deviations of the ions were lower than 5%, and the recovery of the reference materials (GBW08606) was 90%–110%.

1.1.3. OC/EC analysis

The concentration of OC and EC were analyzed using a thermal and optical carbon analyzer (DRI Model 2001A). The analyzer was calibrated through the standard sucrose solutions for quality control. Duplicate punches of each sample were applied to remove the effects of the non-uniformity depositions on the filter. About 10% of total samples were selected to conduct the replicate analyses, and the differences implicated by replicate analyses were within 10% for OC and EC.

1.1.4. Elemental analysis

Half of each sample (blank filter) was digested at 170°C for 4 hr in a Teflon tube with 3 mL of HNO_3, 1 mL of HF, and 1 mL of HCl. The solutions were dried after cooling, and then diluted to 10 mL using distilled deionized water. A total of 20 trace elements were measured using inductively coupled plasma-mass spectrograph (ICP-MS) and inductively coupled plasma-atomic emission spectrometer (ICP-AES). Based on the measurement of the reference materials (S4400-1000241) and the repeated samples, the relative standard deviation was below 3%. The recovery of the reference materials ranged from 95% to 105%.

1.1.5. Scanning electron microscope/TEM analysis

The aerosol particles collected on the TEM grids were observed using a JEOL-2010F field emission high-resolution TEM (FE-HRTEM) combined with an Oxford energy-dispersive X-ray spectrometer (EDS) to obtain the morphology and composition of particles at a single-particle level. EDS spectra were recorded in a TEM image mode and quantified using ES Vision software. EDS were sampled for only 30 sec so that it could weaken radiation exposure. Four areas were selected from the center to the periphery on each grid in order to ensure that the analyzed particles could represent the entire size range. High resolution TEM (HRTEM) was also performed to determine the crystalline structure of particles (S. Guo et al., 2014; L. Guo et al., 2014; H.B. Fu et al., 2014; X.X. Fu et al., 2014).

The morphology and chemistry components of the individual particles were also analyzed using a JEOL JSM 6300 SEM, coupled with an Oxford EDS. SEM runs at the accelerating voltage of 20 kV with a beam current 50–100 nA.

1.2. Statistical analysis

One-way ANOVA (Fisher Test, $p < 0.05$) was used to identify the significant difference of gaseous pollutants, VOCs, and PM concentrations during the different periods. Pearson correlation analysis was used to identify the relationship between meteorological factor and particle volume concentration. All of statistical analysis and figures in this study were performed by the software package SPSS 16.0 and Origin 8.0 for Windows.

2. Results and discussion

2.1. Diurnal variation of CO, SO_2 and NO_x inside the tunnel

Traffic volume as a function of time during the monitoring period is shown in Fig. 2. As can be seen that the traffic volume in the

daytime (07:30–20:30 hr) was significantly higher than that at night (20:30–7:30) ($p < 0.05$). In the daytime (07:30–20:30), the mean traffic volume was 2204 vehicles every hour, and the maximum value reached 2656 vehicles between 15:30 and 16:30 hr. The traffic volume declined at night with the lowest value of 426 vehicles during the period of 3:30–4:30 (Fig. 1).

The mean concentrations of CO, SO_2 and NO_x inside and outside the tunnel are illustrated in Fig. 2. The mean concentrations of CO and SO_2 inside the tunnel were 5.59 ppm and 0.04 ppm, both of which were higher by about 8 and 1.5 times than those outside the tunnel, respectively. It was supposed that traffic volume inside and outside the tunnel played an important role on the emissions of the gaseous pollutants (Zhou et al., 2014). Furthermore, the open environment outside the tunnel was more beneficial to the diffusion of the gaseous pollutants than the semi-closed microenvironment of the tunnel. The mean concentration of NO inside the tunnel was 0.67 ppm, which was 9.6 times higher than that outside the tunnel. Aside from the mentioned reason above, NO could also react quickly with O_3 to form NO_2 (Zhou et al., 2014). The O_3 concentration was much lower inside the tunnel in the general situation, suggesting that a small portion of NO was oxidized to NO_2, thus leading to the NO accumulation inside the tunnel. In contrast, the amount of NO oxidized to NO_2 was higher by far outside the tunnel because O_3 was inclined to form under the irradiation. Therefore, a marked difference in the concentration of NO emerged inside and outside the tunnel. Photochemical process of NO contributed to the higher NO_2 concentrations outside the tunnel, which reduced the difference of NO_2 inside and outside the tunnel. Hence, the relative deviation of NO_2 was significantly lower than that of NO inside and outside the tunnel.

Hourly variations of these pollutants inside and outside the tunnel are also shown in Fig. 2. No significantly diurnal variations of the gaseous pollutants except SO_2 in the concentration outside the tunnel were observed. In contrast, the concentration of the gaseous pollutants inside the tunnel displayed the marked diurnal variation. Higher CO concentrations inside the tunnel both appeared in the morning rush hours (6:30–10:30) and evening rush hours (17:30–19:30), whereas they declined to the lowest value at night. As the products of incomplete combustion of gasoline and/or diesel emitted from vehicle engine, CO was widely used as an indicator to assess the performance of the ventilation system. Kristensson et al. (2004) also observed higher concentrations of CO occurring in the morning rush hours and evening rush hours, and thus concluded that its emission was associated with traffic volume. In the present study, traffic volume was positively linked to the CO concentration ($p < 0.05$), suggesting that higher CO concentrations in the morning rush hours and evening rush hours derived from vehicle emissions. Ma et al. (2011) demonstrated that the piston effect significantly affected the CO concentration dispersion especially in a long tunnel, which occurred more frequently at the rush hours. Diurnal variation of SO_2 was similar to that of CO. It was widely acknowledged that SO_2 concentrations were elevated at the rush hours due to vehicle across with the higher number (Ma et al., 2011). Besides, there were a multitude of heavy-duty vehicles feeding diesel travelling through the tunnel at the morning rush hours, which generally released SO_2 because of high sulfur content of diesel fuel (Andrew et al., 2003). Both NO and NO_2 concentrations inside the tunnel displayed similar variation with one of SO_2 and CO, which ranged from 0.20 to 0.88 ppm and 0.83 to 1.46 ppm, respectively. The peaks of NO and NO_2 reached 0.88 and 1.46 ppm at the morning rush hours, and 0.79 and 1.40 ppm at the evening rush hours, respectively, which was probably associated with the traffic volume. One can see the NO_2 concentration varied slightly less than that of NO. It was well known that NO_2 was not the main pollutant emitted directly by vehicles (Alves et al., 2015). NO_x emission in the engine exhaust consisted of 85%–95% of NO and 5%–15% of NO_2 (Ma et al., 2011). In addition, the O_3 concentration was relatively low inside the tunnel so that the amount of NO_2 generated from the reaction of O_3 and NO was less.

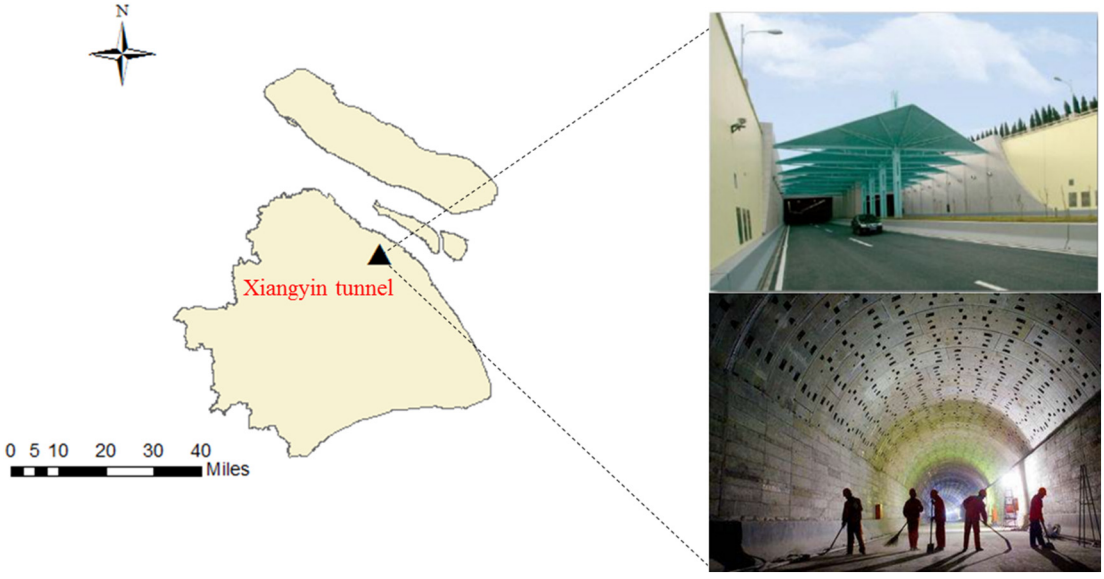

Fig. 1 – The geographical location of Xiangyin tunnel in Shanghai, China.

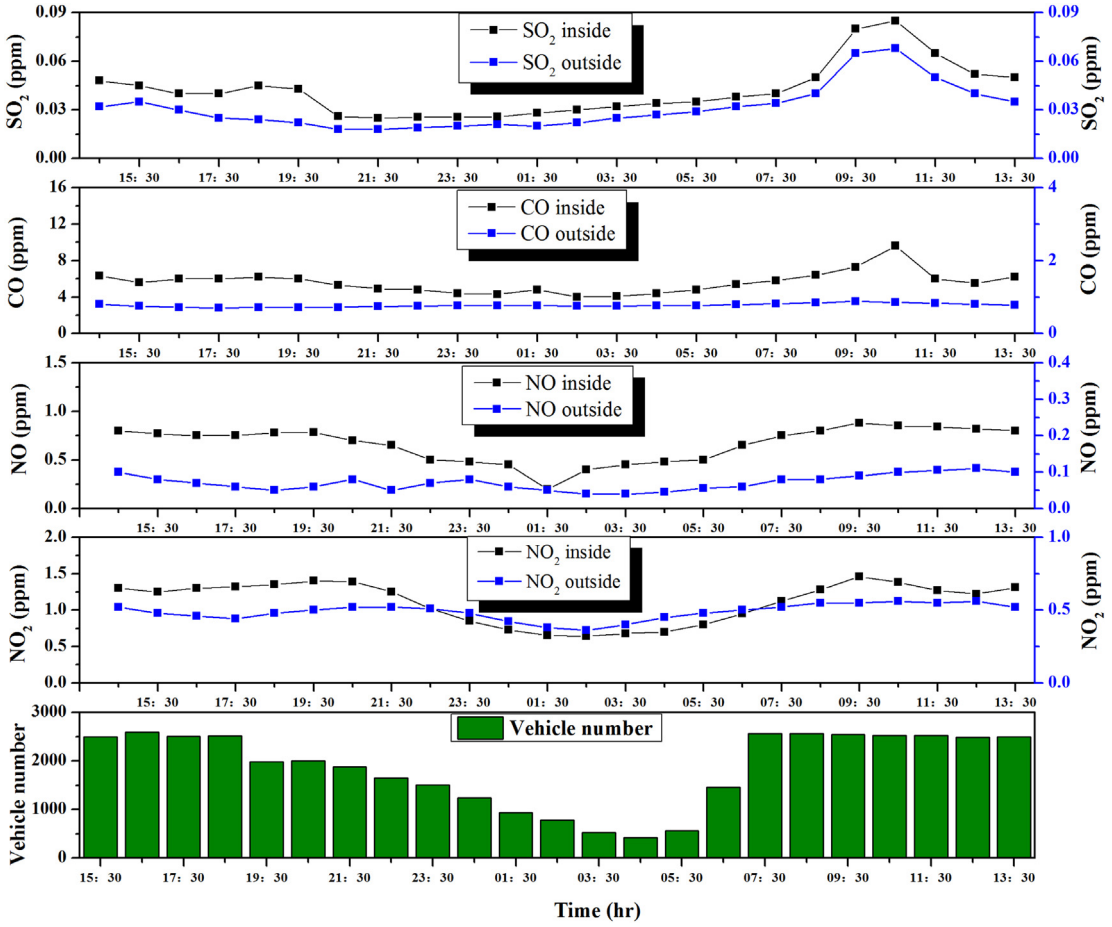

Fig. 2 – Diurnal variation of vehicle number and gaseous pollutant concentrations inside and outside the tunnel.

2.2. Diurnal variation of VOCs inside the tunnel

Fig. 3 shows the main components of VOCs and their diurnal variation inside the tunnel. The a–d periods corresponded to the evening rush hours (17:30–19:30) on 24th, the night (22:30–06:30) on 24th, the morning rush hours (06:30–10:30 hr) on 25th, and noon (11:30–14:30 hr) on 25th, respectively. Diurnal variation of VOCs displayed two peaks at traffic peak hours (morning rush hours: 1698.1 μg/m^3; evening rush hours: 1477.9 μg/m^3). However, the lowest value (648.5 μg/m^3) appeared at night. This diurnal variation was identical to that of CO, SO_2 and NO_x, which could be associated with the traffic volume crossing the tunnel.

Benzene, aliphatic hydrocarbons, methylbenzene, xylene, ethylbenzene, undecane, phenylethylene and butylacetate were major components of VOCs in the tunnel, which was in good agreement with the previous studies (Zhang et al., 2017; Chiang et al., 2007; Ho et al., 2009). The concentrations were in the order of benzene > aliphatic hydrocarbons > methylbenzene > xylene > ethylbenzene > undecane > phenylethylene > butylacetate except high undecane at the evening rush hours. Benzene occupied the biggest loadings of VOCs, accounting for 61.9, 57.9, 75.9 and 61.7% during four different periods, respectively. The proportion of benzene to VOCs in the Xiangyin tunnel was significantly higher than that in some industrial areas, the urban areas and the tunnels observed previously (Chiang et al., 2007; Cai et al., 2010). This was probably associated with higher traffic volume in the Xiangyin tunnel because of higher emission factor of benzene relative to other aromatics in the vehicle exhausts (Duffy and Nelson, 1996). Aliphatic hydrocarbons (15.5%–30.5%) were the second highest group followed by methylbenzene (2.99%–7.73%) and xylene (2.29%–6.59%). The emissions of aliphatic hydrocarbons were mainly originated from evaporative emissions and fuel combustion (Na et al., 2005). Dense passing of heavy-duty and light-duty vehicles seem to have a substantial impact on the elevation of aliphatic hydrocarbons in the tunnel. It was well documented that the use of unleaded fuels decreased the concentrations of lead in the atmosphere sharply, but it increased the emission of methylbenzene because it was generally added to unleaded fuels (Ho et al., 2004). Gasoline evaporation might be additionally attributed to high methylbenzene emission (Na et al., 2003). Apart from a solvent used in coatings, paints, and cleaning agents, xylene was confirmed to be an important component of vehicle exhaust, which was enriched in the effluent of fossil fuels (Chan et al., 2011).

The BTEX species (benzene, methylbenzene, ethylbenzene and xylene) exhibited marked diurnal variation inside the tunnel. The peaks of BTEX at the morning rush hours may

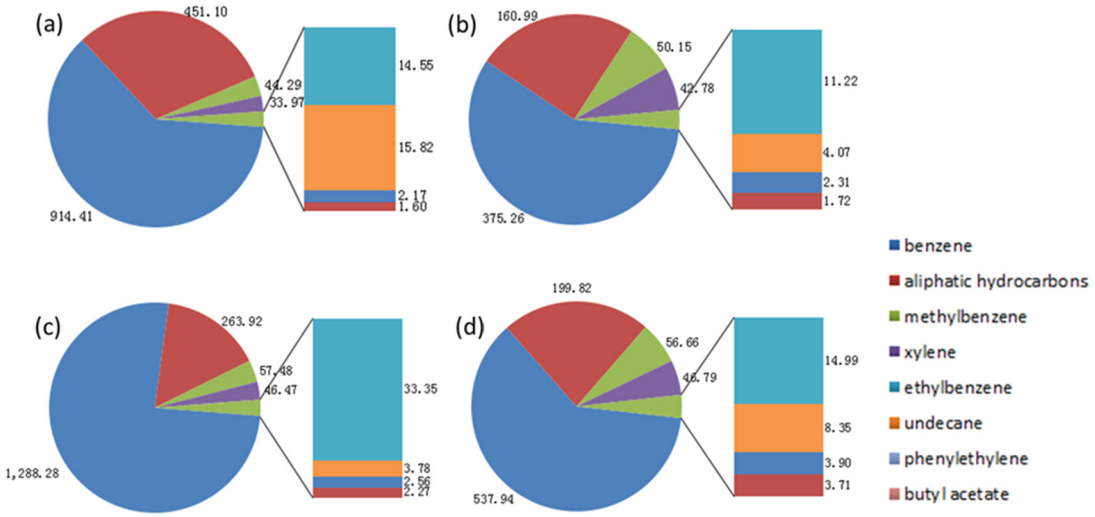

Fig. 3 – Concentrations and compositions of volatile organic compounds (VOCs) during four periods inside the tunnel. (a) night rush hours (17:30–19:30) on April 24th, (b)night (22:30–06:30) in April 24th; (c)morning rush hours (06:30–10:30) in April 25th; (d) noon (11:30–14:30) in April 25th) (Unit: μg/m^3).

result from the high traffic volume. After this period, the concentrations of BTEX started to decrease due to the decrease of traffic volume. During the evening rush hours, BTEX showed higher values in the concentration due to the increase of gasoline vehicles and evaporative emissions (Na et al., 2003). At midnight, BTEX declined to the lowest values due to the decrease of traffic volume. T/B ratio (methylbenzene: benzene) was an indicator to identify the source of VOCs. Higher T/B ratios suggested the increase of gasoline vehicles, but the decrease of diesel vehicles (Ho et al., 2004). Due to the lack of xylene, the X/E ratio was generally lower in the case of diesel vehicle (Ho et al., 2004). The T/B ratios in the four periods ranged from 0.0446 to 0.1336, all of which were rather low in comparison to the other tunnels in Hong Kong, Manila, Bangkok and Korea (Gee and Sollars, 1998; Ho et al., 2004; Na and Kim, 2001). The T/B ratio determined herein may be regarded a characteristic value for the on-road tunnel emissions, suggesting that diesel vehicles were major vehicles passing through the Xiangyin tunnel. The T/B ratio displayed a remarkable diurnal variation. The highest value occurred at night, while it showed a lowest one during the morning rush hours, which was attributed to the different vehicle types. In the case of the Xiangyin tunnel, the X/E ratio displayed two peaks at night (3.81) and at noon (3.12), respectively; whereas it showed the lowest value of 1.39 during the morning rush hours, demonstrating that the proportion of gasoline vehicles passing the tunnel was much higher at night as compared to the other periods.

2.3. Size distribution of PM and their components

2.3.1. Size distribution and diurnal variation of the PM concentration

The mass concentrations of the particles in the different sizes are shown in Fig. 4. The mean concentration of PM_{10} in the tunnel was 224 μg/m^3. Two peaks of PM in the concentration appeared in both $PM_{0.7–1.1}$ and $PM_{3.3–4.7}$ fractions, respectively. The proportion of $PM_{1.1}/PM_{10}$, $PM_{2.1}/PM_{10}$ and $PM_{1.1}/PM_{2.1}$ inside the tunnel was about 22.9%, 34.7% and 66.0%, respectively.

2.3.2. Size distribution of the components in the PM

The size distributions of water-soluble ions (*e.g.*, SO_4^{2-}, NO_3^-, Cl^-, NH_4^+, *etc.*), OM and EC measured are summarized in Fig. 4. The OM concentration was expressed as 1.2 × OC in our study (Harrison et al., 2003). OM constituted major fraction of the PM mass in the tunnel based on the previous study (Allen et al., 2001). The highest value of OM primarily existed in fine particles (0.7–1.1 μm) at the morning rush hours. Allen et al. (2001) also reported that OM peaked in the fine particles and attributed them to engine exhaust. OM also displayed a slight peak in the coarse particles such as $PM_{5.8–9}$ especially at night, which was originated from mechanical abrasion since about 30% of brake pads were made of carbon (Pio et al. 2013). Alves et al. (2015) reported that the ratio of EC/PM_{10} decreased with the increasing particle size in the Liberdade tunnel, and concluded that EC should be emitted through vehicle tailpipes. However, the EC concentration possessed higher values in the coarse particles in the Xiangyin tunnel, which was probably linked with the incomplete combustion at the condition of the motor vehicles idling in the tunnel because of traffic jam during the rush hours. (Laschober et al., 2004).

The concentrations of the water-soluble ions were generally higher in the fraction of $PM_{2.1–4.7}$. As one of main water-soluble ions, sulfate tended to concentrate in fine particles and was generally correlated with the sulfur contents in fuel, especially those in diesel fuel (Lowenthal et al., 1994). The NH_4^+ emission predominately stemmed from automobiles because they were equipped with catalysts and rich operating fuel (Allen et al., 2001). Besides, the emission of aerosol NH_4^+ also probably stem *via* a second process from the reaction of gas-phase NH_3 in the tunnel (Allen et al., 2001). NO_3^- was also an important water-soluble ion, concentrated in the fine particles such as $PM_{2.1}$. Vehicle exhaust was a major contribution

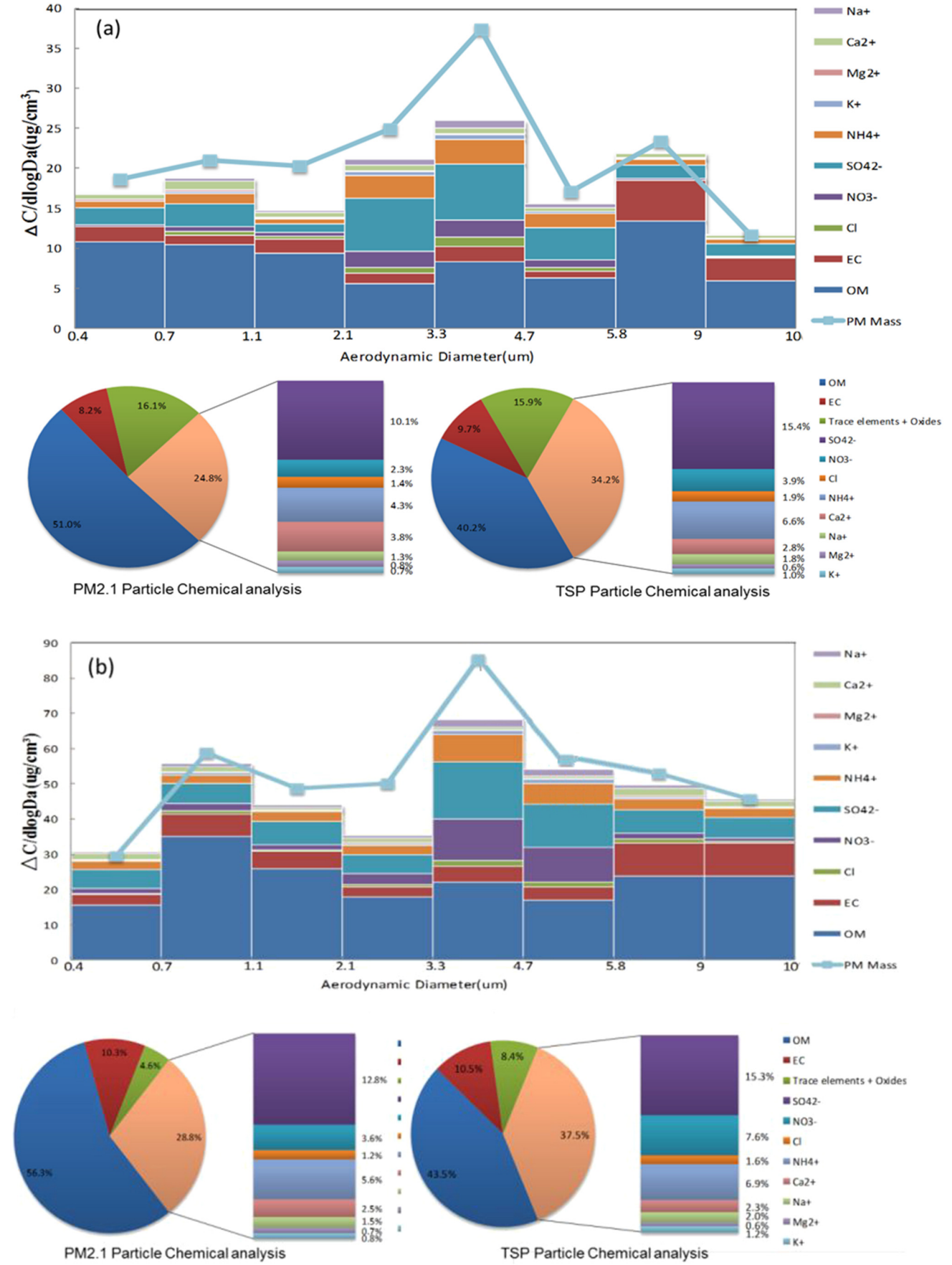

Fig. 4 – Mean concentration and composition of PM during the morning rush hours and at night. (a) night, (b) morning rush hours. PM; particulate matter.

of NO_x emissions in China. NO_3^- could be transformed from NO_x, nitrous acid (HONO), and organic nitrates (*i.e.*, $RONO_2$) (H.B. Fu et al., 2014; X.X. Fu et al., 2014). Both NO and NO_2 concentrations were higher inside the Xiangyin tunnel, thereby elevating the concentrations of NO_3^-. Ca^{2+}, Na^+, Mg^{2+}, K^+ and Cl^- were also main ions hosted by the particles. The proportion of Na^+ and Mg^{2+} in 3.3–5.8 μm was significantly higher than that in the ultrafine particles. It was assumed that both Na^+ and Mg^{2+} especially in the coarse particles (4.7–5.8 μm) were predominately derived from bedrock weathering and resuspension of dust (Pio et al., 2013). Besides, a small quantity of Na^+ and Mg^{2+} in PM could be also sourced from the remains after the evaporation of sea-salt. Furthermore, Na^+/Mg^{2+} ratio in the coarse particles were in the ranged of 2–3, similar to that of ocean water (Pio et al., 2013). Calcium was main crustal element, as well as sodium and magnesium, primarily concentrated in the coarse particles. In the present study, the highest Ca^{2+} concentration accumulated in the size range of 5.8–9.0 μm in the Xiangyin tunnel, implicating natural source possibly. Apart from the impacts of natural contribution, Ca^{2+} in the find mode could also originate from vehicle exhaust (Ault et al., 2012). Furthermore, Ca^{2+} was also thought to stem from the cement dusts of construction sites (Hu et al., 2015). It is well known that calcite is frequently used as filler in concrete, and portlandite is a normal reaction product in concrete (Kaegi, 2004). Li et al. (2008) concluded that Ca-rich particles in the fly ash of cement predominately peaked in coarse particles. Although K^+ was generally recognized as a fingerprint of biomass burning, no obvious biomass burning was observed around the tunnel (Pio et al., 2013). It was well known that K^+ and Cl^- were also likely derived from the re-suspended dust (Hays et al., 2005).

2.3.3. *Diurnal variation of the main components in the PM*

The concentrations of OM, EC and some water-soluble ions (*e.g.*, SO_4^{2-}, NO_3^-, NH_4^+, K^+, Ca^{2+}, Na^+, *etc.*) in each stage were elevated during the morning rush hours as compared to those at night (Fig. 4). The percentages of diesel vehicles were generally higher during the morning rush hours than that at night, and thus increased the emissions of OM and EC (Cui et al., 2016). The OC/EC value was not only used as an indicator to estimate the contribution of vehicle emissions to carbonaceous aerosol in the atmosphere (Gelencsér et al., 2007), but also was a good tracer to identify gasoline vehicle emission from diesel vehicle one. The OC/EC ratio generally decreased with the increasing of diesel vehicles especially in a semi-close environment, such as tunnel (Liu et al., 2012). The OC/EC ratio in $PM_{2.1}$ and TSP were 2.96 and 1.68 in the morning, and 3.66 and 3.29 at night, respectively, which was caused by high proportion of diesel vehicles passing through in the Xiangyin tunnel in the morning (Gillies et al., 2001). The concentrations of SO_4^{2-} and NO_3^- displayed similar diurnal variation to OM and EC because they correlated significantly with sulfur and nitrogen contents in diesel fuel, respectively (Lowenthal et al., 1994). The NO_3^-/SO_4^{2-} ratio could reflect the contribution of stationary and mobile sources to sulfur and nitrogen in the atmosphere, which elevated with the increasing of mobile sources (H.B. Fu et al., 2014; X.X. Fu et al., 2014). In our study, the NO_3^-/SO_4^{2-} ratio increased from night ($PM_{2.1}$: 0.23, TSP: 0.25) to the morning rush hours ($PM_{2.1}$: 0.28, TSP: 0.49), implying the contribution of traffic volume. NH_4^+ featured a similar diurnal variation with SO_4^{2-} and NO_3^-, indicating possibly the presence of $(NH_4)_2SO_4$ and NH_4NO_3 (Gao et al., 2011). K^+ showed slightly higher value during the morning rush hours than that at night, suggesting more frequent dust resuspension when large amounts of vehicles pass through the tunnel (Pio et al., 2013). The diurnal variations of Na^+, Mg^{2+}, and Ca^{2+} were identical to K^+, which was ascribed to that the number of heavy-duty vehicles crossing the tunnels was higher in the daytime, induced more mineral element resuspension (Cui et al., 2016).

2.4. *Number concentrations and size distribution of the particles*

The diurnal variations of meteorological factors, and number concentrations, surface concentrations, and volume concentrations of particles are depicted in Fig. 5. Air temperature displayed homogeneous variation between 14:30 and 6:30, whereas it increased significantly during the morning rush hours. The variation of relative humidity was contrary to those of air temperature (Fig. 5a). Markedly diurnal variation of number concentrations, surface concentrations, and volume concentrations were observed. The peaks of particle number concentrations reached around 2–3 × 10^5/cm^3 during the morning rush hours (Fig. 5b) due to the high traffic volume during that period. After this period, the particle concentration started to decrease due to the decrease of traffic volume. Particle number concentration declined to a lowest value of about 5 × 10^4/cm^3 at 22:30. Particle surface concentration, and volume concentration exhibited similar diurnal variation to particle number concentrations.

The diurnal variation of particle number concentration in different particle diameters is depicted in Fig. S1. Particle number concentration exhibited three peaks in Aitken mode (25 nm and 100 nm) and accumulation mode (600 nm), respectively, which was in agreement with previous research reported by Abu-Allaban et al. (2002). The particle number concentration in Aitken mode was markedly higher during the morning rush hours than that at night. There may be two reasons accounting for such results. Firstly, particles in Aitken mode were likely emitted through the exhaust pipes since the peak of particle number concentration was similar to the peak of vehicle exhausts (20–80 nm) (Pirjola et al., 2004), which was usually associated with the variation of traffic volume. Secondly, lower ambient temperature and higher RH during the morning rush hours easily lead to the formation of Aitken mode (Ristovski et al., 1998). It was widely acknowledged that the particles in Aitken mode originated from vehicle exhaust, which generally condensed quickly at low temperature or formed through nucleation and growth (Harris and Maricq, 2001; Ristovski et al., 1998). Apart from the peak in Aitken mode, there was a small peak in the accumulation mode around 600 nm. These particles were probably formed through the accumulation of ultrafine particles or coagulation and then growth by adsorption of gaseous pollutants (Harris and Maricq, 2001).

The diurnal variation of particle volume concentration is summarized in Fig. S2. Particle volume concentration exhibited the high values at accumulation mode (100–500 nm) and

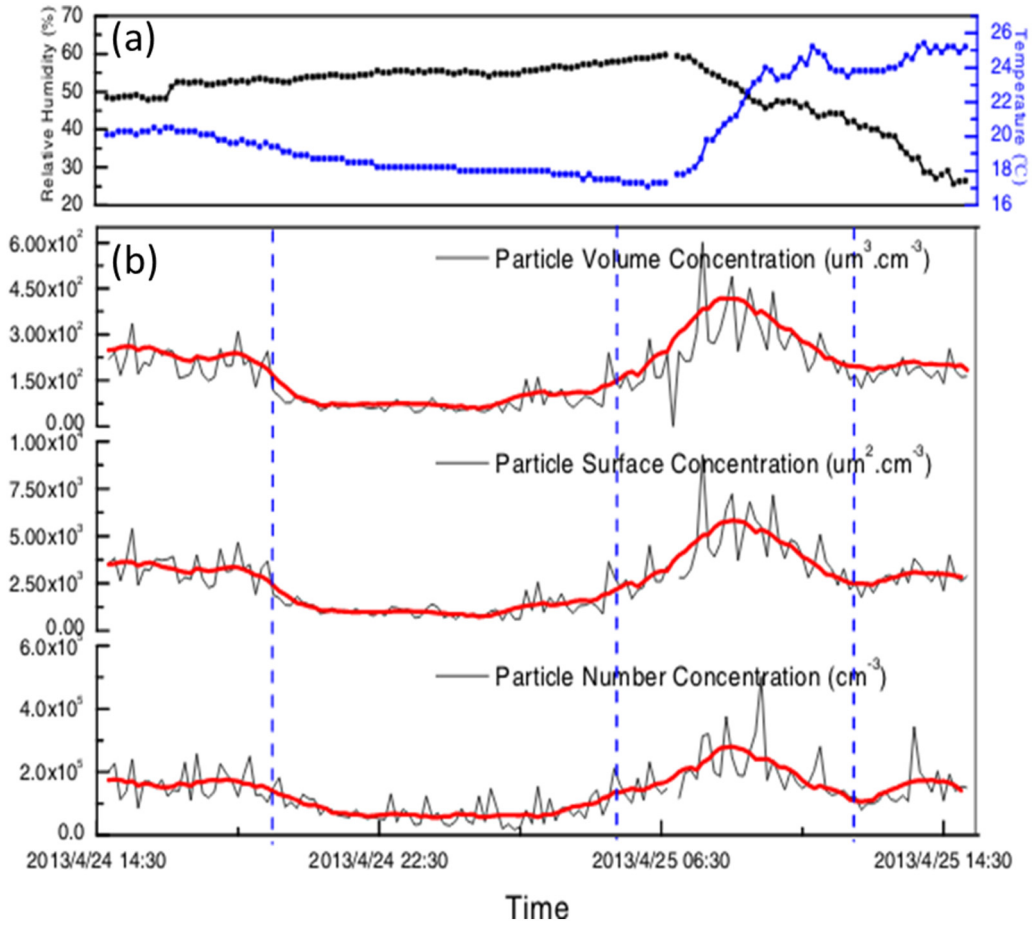

Fig. 5 – Diurnal variation of meteorological factors, particle number concentration, surface concentration and volume concentration inside the tunnel.

coarse mode (2.5–4.0 μm). Coarse mode particles may form *via* three ways: direct particle emissions from vehicles, re-suspension of dusts, or the evaporation of larger droplets (Meng and Seinfeld, 1994). RH and the particles in the size range of 2.5–4.0 μm displayed an insignificantly correlation ($r = 0.28$, $p > 0.05$), suggesting that larger droplets did not play a significant role in the formation of coarse particles in the tunnel. Particles directly emitted by vehicle exhaust generally displayed high values at nucleation mode and Aitken mode (Alves et al., 2015). Therefore, we finally supposed the particles with the sizes of 2.5–4.0 μm may originate from the resuspension of dusts. In the present research, most of particles were concentrated in the mass median diameter (MMD) of 0.33 ± 0.06 μm. In accordance with the number concentration, the volume concentrations of particles for all diameters showed the significantly positive relationship to traffic volume, suggesting that vehicle emissions were the main source of PM in the tunnel.

Particle size distributions during five periods are shown in Fig. 6. Two peaks (25 nm and 100 nm) could be observed in the morning and afternoon, whereas the peak at 100 nm diminished in the evening. It was documented that the diameter of diesel engine combustion particles ranged from 60 to 120 nm, but those from a gasoline engine exhaust tend to range from 40 to 80 nm (Woo et al., 2001). The proportion of diesel vehicles was much higher in the daytime than that at night on the basis of the previous analysis. Besides, the peak at 100 nm was often formed through coagulation and growth of ultrafine particles existed in the atmosphere (Wehner and Wiedensohler, 2003).

2.5. *Morphology and speciation of the particles collected from the tunnel*

Five categories of the particles collected from the tunnel have been differentiated under the SEM: Fe-rich particles, mineral particles, EC, Ca–S mixtures and Al–Si particles (shown in Fig. S3) and Fig. 7. Fe-rich particles and mineral particles were mainly characterized by irregular shape, EC showed a typical chain-like shape, Ca–S mixtures displayed a bar-like shape, and Al–Si particles presented a smooth spherical morphology. The relative abundance of mineral particles was higher at night than that during other periods owing to fewer vehicles at night.

The typical Fe-rich particles, K-rich particles, mineral particles, Ca–S particles and Al–Si particles are shown in Fig. 8, accounting for 34%, 21%, 11%, 7% and 1%, respectively. The fine Fe-rich particles were mainly composed of iron

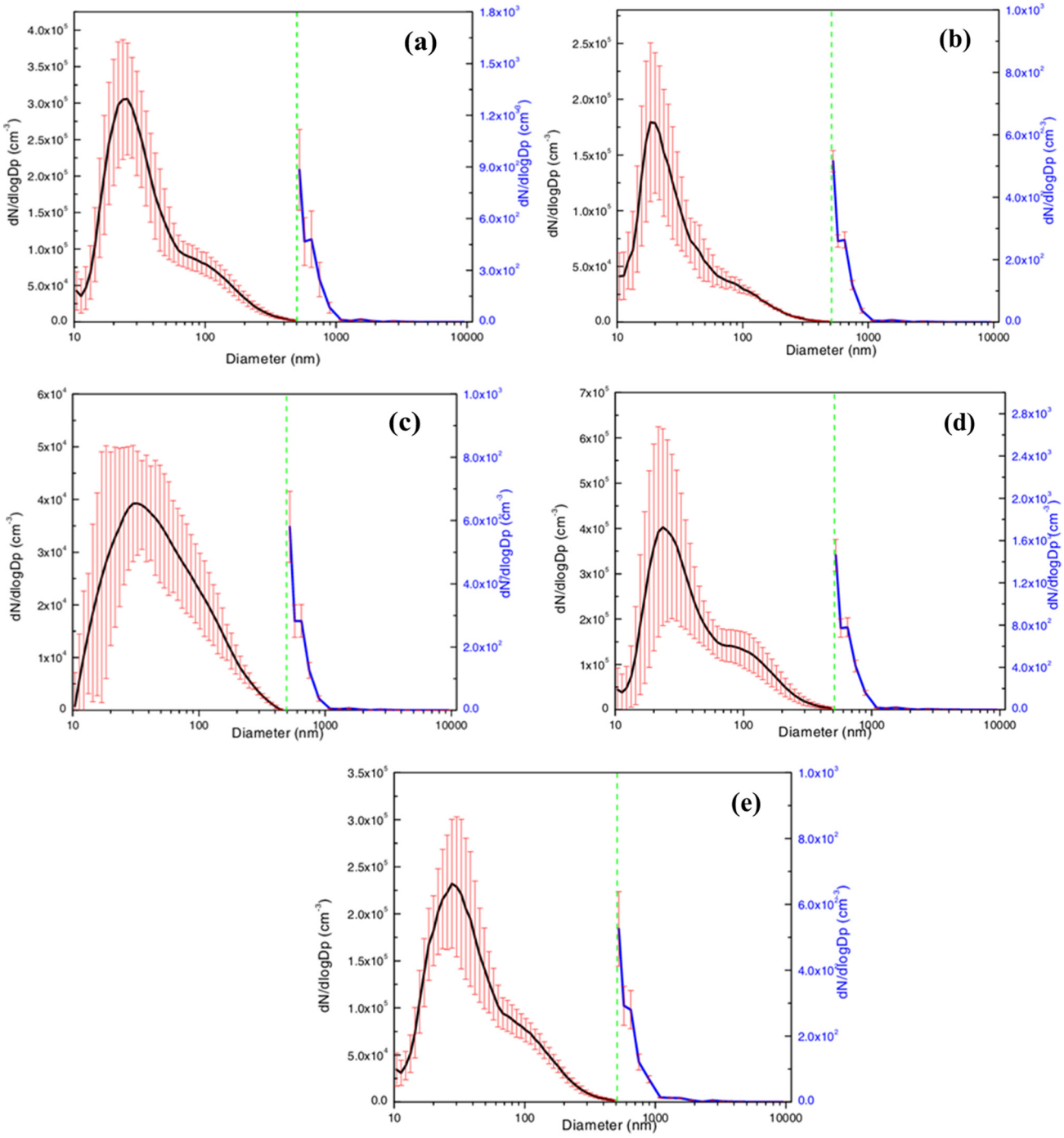

Fig. 6 – Size distribution of particles during different periods inside the tunnel (a: 17:00 hr in 24th, b: 20:00 hr in 24th, c: 3:00 hr in 25th, d: 9:00 hr in 25th, e: 13:00 hr in 25th).

oxides, which was characterized by darker color due to the condensation of OM (S. Guo et al., 2014; L. Guo et al., 2014). Fe-rich particles were generally mixed with crustal elements, such as Si, Ca, Al and Mg, as well as some trace metals, such as Ba and Zn. Both Ba and Zn were regarded as the good fingerprints of abrasive and tire dust. (Hjortenkrans et al., 2007; Alves et al., 2015). Kang et al. (2008) concluded that Fe-rich particles probably stemmed from mechanical wear of brake and tyres. EDS data showed that Al–Si particles with spherical shape contained high concentrations of Fe and O with low Ba content. The particle with sphere morphology was common generated from a gas-to-particle transformation followed by condensational growth under high-temperature environment (Ault et al., 2012). Furthermore, Ba was widely used as a tracer of the traffic origin. Thus, Al–Si particles were probably emitted by vehicle exhaust. In the most case, the Fe–containing particles were inclined to form nanosphere aggregates, and internally mixed with EC. The high fraction of EC

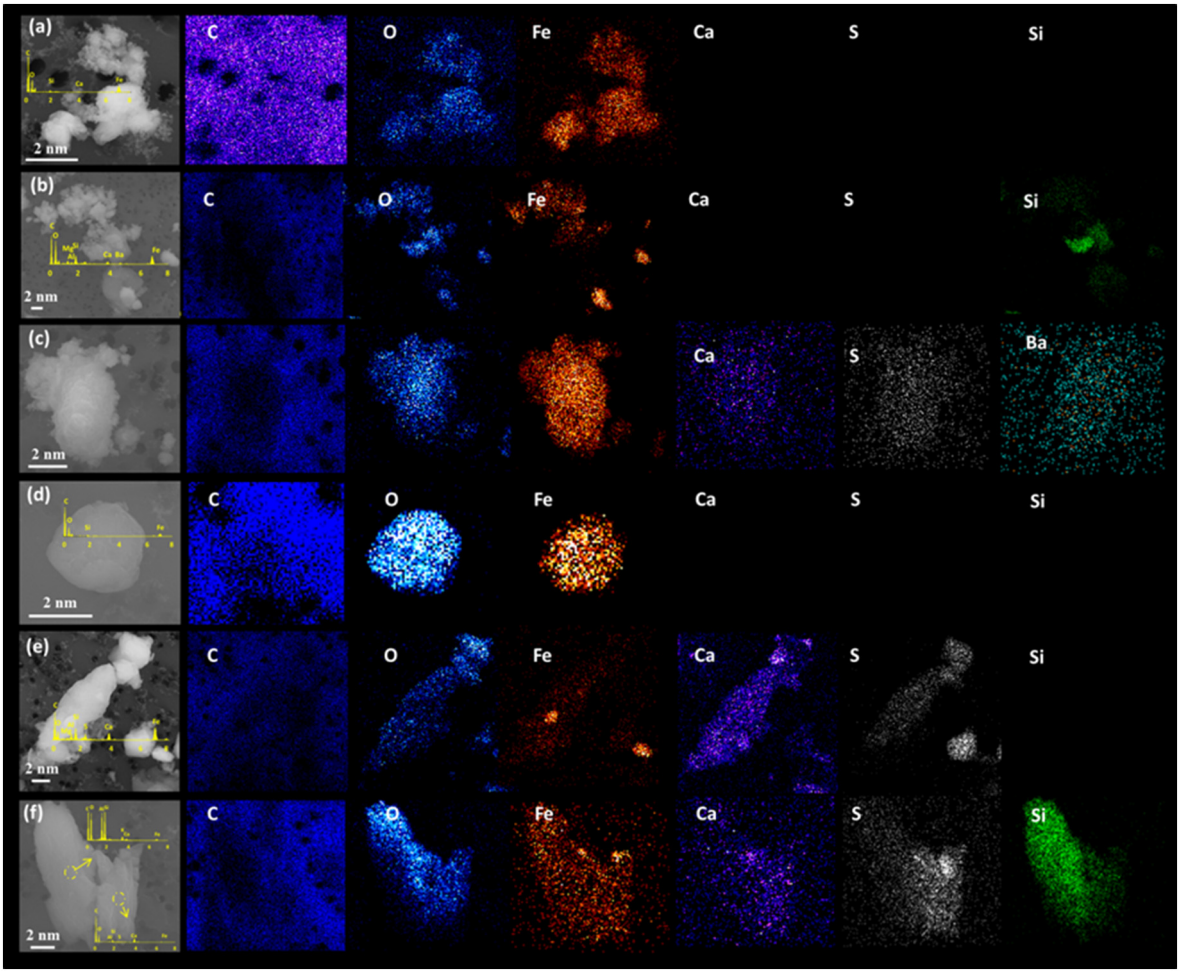

Fig. 7 – SEM images and elemental distribution maps of typical particles. (a–c) Fe-rich particles; (d) organic matter; (e) Ca–S particles; (f) mineral dust. SEM: scanning electron microscope.

would be contributed when the vehicle ran under high load (Alves et al., 2015). Aside from the mixture of Al–Si particlesand EC, K-rich particles were often internally mixed with EC under the TEM.

The mineral dusts displayed a great deal of variability in composition, generally classified into two kinds: silicate-rich and calcium-rich minerals, which exhibited lighter colors in contrast to Fe-rich particles under the TEM. Silicate and calcium were main components of quartz, feldspar and mica, all of which could release these crustal elements through physical, chemical or biological weathering and consequent resuspension processes (Cwiertny et al., 2008). Pio et al. (2013) concluded that Si and Ca usually reflected the origin of road dust resuspension and mechanical disaggregation of road surface.

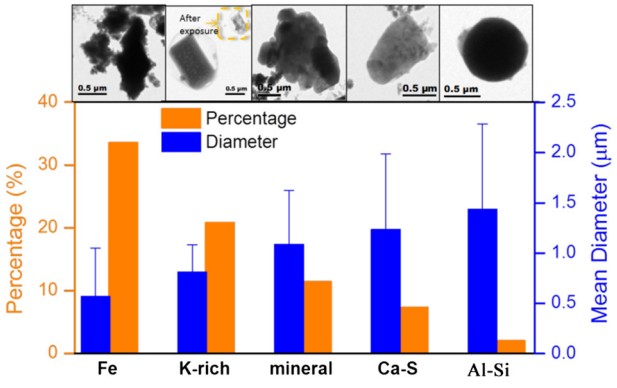

Fig. 8 – Relative abundance and size distribution of main components of single particles.

Ca–S particles were more prone to being contributed by local sources, such as industrial activities (Kodavanti et al., 1998). during the recent past years, desulfurization of SO_2 by CaO was widely applied to improve air quality in many cities, which was rewarding to the formation of Ca–S particles. Apart from the impacts of industrial activities, the Xiangyin tunnel was more or less affected by the construction source because many business streets were being built during the sampling period.

The element concentrations exhibited marked differentiation between the rush hours and non-rush hours (Fig. 9). Al, Fe, S, Si and Zn elements were higher during the rush hours than those during the non-rush hours, which were in agreement with the results in the other tunnels (Brito et al., 2013). Al and Si were mainly originated from road dusts re-

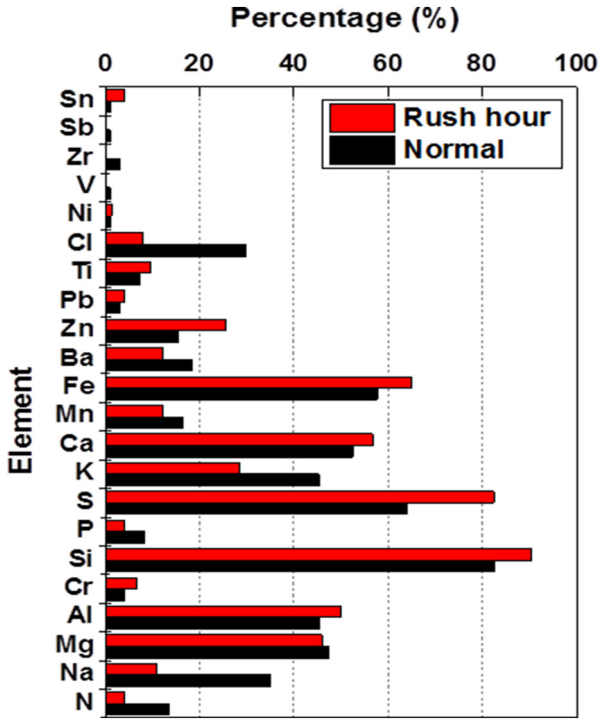

Fig. 9 – Elemental compositions of particles inside the tunnel analyzed by TEM-EDS. TEM: transmission electron microscopy; EDS: energy-dispersive X-ray spectrometer.

suspension (Da Silva et al., 2010), whereas Fe and Zn were emitted by mechanical processes (*e.g.*, wear of brakes and tyres). Sulfur was generally associated with other materials, such as insoluble barite, a major constituent of brake pads (Querol et al., 2008). Thus, Al, Fe, S, Si and Zn in the atmospheric particles displayed similar variation with traffic volume.

2.6. *Uncertainty*

Although some of the results in our study were in agree with some previous studies, there were still some uncertainties with regard to the tunnel studies. First, the particles outside the tunnel could influence the accumulation of particles inside the tunnel. For instance, Na^+ and Cl^- could be transported to Xiangyin tunnel through strong advection because Xiangyin tunnel was close to the East China Sea. In addition, only a working day was selected to perform the study in the tunnel. Despite no significant difference in the weekdays, the weekly variation of vehicle emissions cannot be elucidated in our study.

3. Conclusions

Both gaseous pollutants and PM exhibited higher values during the morning and evening rush hours due to vehicle emissions. Two peaks of the PM concentrations were observed in $PM_{0.7–1.1}$ and $PM_{3.3–4.7}$ fractions. OM was mainly concentrated in the fine particles, whereas the concentrations of EC peaked in the coarse particles because some vehicles idled in the tunnel. Most of water-soluble ions (except Na^+, Mg^{2+} and Ca^{2+}) displayed the highest values in $PM_{2.1–4.7}$. The accumulation of Na^+, Mg^{2+}, K^+, and Cl^- were originated from dust suspension, while Ca^{2+} may be sourced from consumption of cement. The concentrations of OM, EC, and nearly all water-soluble ions (including SO_4^{2-}, NO_3^-, NH_4^+, Na^+, Mg^{2+}, K^+, Cl^-, and Ca^{2+}) were markedly higher during the morning rush hours than those at night, implying the effects of vehicle types, traffic volume and/or meteorological factors. Particle number concentrations achieved a peak value with 2–3 × 10^5/cm^3 in the morning rush hours, whereas they declined to the lowest value of 5 × 10^4/cm^3 at night. The particle number concentration exhibited two peaks at Aitken mode (25 nm and 100 nm) and accumulation mode (600 nm), while the particle volume concentration displayed high values at accumulation mode (100–500 nm) and coarse mode (2.5–4.0 μm), which was associated with the vehicle emissions, as well as nucleation and growth of particles. The peak around 100 nm was detected in the morning rush hours, but it diminished with the decrease of traffic volume. TEM analysis revealed that main particles in the tunnel were Fe-rich particles, K-rich particles, BC, mineral particles, Ca–S rich particles and Al–Si particles. The morphology of the tunnel particles exhibited difference in the element concentrations and particle size between the rush and non-rush period. This research will shed a light on the impacts of tunnel to the air quality and public health.

Acknowledgments

This work was supported by the National Key R&D Program of China (2016YFC0202700), Ministry of Science and Technology of China (2016YFE0112200), National Natural Science Foundation of China (Nos. 21777025, 21577022, 21190053, 40975074), the Marie Skłodowska-Curie Actions (690958-MARSU-RISE-2015) and the International Cooperation project of Shanghai municipal government (15520711200).

Appendix A. Supplementary data

Supplementary data to this article can be found online at https://doi.org/10.1016/j.jes.2017.11.015.

REFERENCES

Abu-Allaban, M., Coulomb, M., Gertler, A.W., Gillies, J., Pierson, W. R., Rogers, C.F., et al., 2002. Exhaust particle size distribution measurements at the tuscarora mountain tunnel. Aerosol Sci. Technol. 36, 771–789.

Adar, S.D., Gold, D.R., Coull, B.A., Schwartz, J., Stone, P.H., Suh, H., 2007. Focused exposures to airborne traffic particles and heart rate variability in the elderly. Epidemiology 18, 95–103.

Allen, J.O., Mayo, P.R., Hughes, L.S., Salmon, L.G., Cass, G.R., 2001. Emissions of size-segregated aerosols from on-road vehicles in the Caldecott Tunnel. Environ. Sci. Technol. 35, 4189–4197.

Alves, C.A., Gomes, J., Nunes, T., Duarte, M., Calvo, A., Custódio, D., 2015. Size-segregated particulate matter and gaseous emissions from motor vehicles in a road tunnel. Atmos. Res. 153, 134–144.

Andrew, J.K., Robert, A.H., Gary, R.K., 2003. Effects of vehicle speed and engine load on motor vehicle emissions. Environ. Sci. Technol. 10, 3739–3746.

Anenberg, S.C., Schwartz, J., Shindell, D.T., Amann, M., Faluvegi, G. S., Klimont, Z., 2012. Global air quality and health co-benefits of mitigating near-term climate change through methane and black carbon emission controls. NASA Tecnical Report 120, pp. 831–839.

Ault, A.P., Peters, T.M., Sawvel, E.J., Casuccio, G.S., Willis, R.D., Norris, G.A., 2012. Single-particle SEM-EDX analysis of iron-containing coarse particulate matter in an urban environment: Sources and distribution of iron within Cleveland, Ohio. Environ. Sci. Technol. 46, 4331–4339.

Brito, J., Rizzo, L.V., Herckes, P., Vasconcellos, C., Caumo, S., Fornaro, A., 2013. Physical-chemical characterisation of the particulate matter inside two road tunnels in the São Paulo Metropolitan Area. Atmos. Chem. Phys. 13, 12199–12213.

Cai, C.J., Geng, F.H., Tie, X.X., Yu, Q., An, J.L., 2010. Characteristics and source apportionment of VOCs measured in Shanghai, China. Atmos. Environ. 44, 5005–5014.

Chan, Y.C., Hawas, O., Hawker, D., Vowles, P., Cohen, D.D., Stelcer, E., Simpson, R., Golding, G., Christensen, E., 2011. Using multiple type composition data and wind data in PMF analysis to apportion and locate sources of air pollutants. Atmos. Environ. 45, 439–449.

Chiang, H.L., Huang, Y.S., 2009. Particulate matter emissions from on-road vehicles in a freeway tunnel study. Atmos. Environ. 43, 4014–4022.

Chiang, H.L., Hwu, C.S., Shih-Yu, C., Chen, S.Y., Wu, M.C., Ma, S.Y., Huang, Y.S., 2007. Emission factors and characteristics of criteria pollutants and volatile organic compounds (VOCs) in a freeway tunnel study. Sci. Total Environ. 381, 200–211.

Cui, M., Cheng, Y.J., Tian, C.G., Zhang, F., Yan, C.Q., Zheng, M., 2016. Chemical composition of $PM_{2.5}$ from two tunnels with different vehicular fleet characteristics. Sci. Total Environ. 550, 123–132.

Cwiertny, D.M., Baltrusaitis, J., Hunter, G.J., Laskin, A., Scherer, M. M., Grassian, V.H., 2008. Characterization and acid-mobilization study of iron-containing mineral dust source materials. J. Geophys. Res. 113, D05202.

Da-Silva, M.F., De-Assuṇão, J.V., Andrade, M.D.F., Pesquero, C.R., De, Kempinas, Barbosa, W.G., Júnior, F., 2010. Characterization of metal and trace element contents of particulate matter (PM_{10}) emitted by vehicles running on Brazilian fuels-hydrated ethanol and gasoline with 22% of anhydrous ethanol. J. Toxicol. Environ. Health A 73, 901–909.

Duffy, B.L., Nelson, P.F., 1996. Non-methane exhaust composition in the Sydney Harbour Tunnel: a focus on benzene and 1, 3-butadiene. Atmos. Environ. 30, 2759–2768.

El-Fadel, M., Hashisho, Z., 2001. Vehicular emissions in roadway tunnels: a critical review. Crit. Rev. Environ. Sci. Technol. 31, 125–174.

Fu, X., Wang, S.X., Zhao, B., Xing, J., Cheng, Z., Liu, H., Hao, J.M., 2013. Emission inventory of primary pollutants and chemical speciation in 2010 for the Yangtze River Delta region, China. Atmos. Environ. 70, 39–50.

Fu, H.B., Shang, G.F., Lin, J., Hu, Y.J., Hu, Q.Q., Guo, L., Zhang, Y.C., Chen, J.M., 2014a. Fractional iron solubility of aerosol particles enhanced by biomass burning and ship emission in Shanghai, East China. Sci. Total Environ. 481, 377–391.

Fu, X.X., Wang, X.M., Guo, H., Cheung, K., Ding, X., Zhao, X.Y., 2014b. Trends of ambient fine particles and major chemical components in the Pearl River Delta region: observation at a regional background site in fall and winter. Sci. Total Environ. 432, 274–281.

Gao, X.M., Yang, L.X., Cheng, S.H., Gao, R., Zhou, Y., Xue, L.K., 2011. Semi-continuous measurement of water-soluble ions in $PM_{2.5}$ in Jinan, China: temporal variations and source apportionments. Atmos. Environ. 45, 6048–6056.

Gee, I.L., Sollars, C.J., 1998. Ambient air levels of volatile organic compounds in Latin American and Asian cities. Chemosphere 36, 2497–2506.

Gelencsér, A., May, B., Simpson, D., Sánchez-Ochoa, A., Kasper-Giebl, A., Puxbaum, H., 2007. Source apportionment of $PM_{2.5}$ organic aerosol over Europe: primary/secondary, natural/anthropogenic, and fossil/biogenic origin. J. Geophys. Res. 112 (D23).

Gillies, J., Gertler, A., Sagebiel, J., Dippel, N.W., 2001. On-road particulate matter ($PM_{2.5}$ and PM_{10}) emissions in the Sepulveda Tunnel, Los Angeles, California. Environ. Sci. Technol. 35, 1054–1063.

Guo, S., Hu, M., Zamora, M.L., Peng, J.F., Shang, D.J., Zheng, J., 2014a. Elucidating severe urban haze formation in China. Proc. Natl. Acad. Sci. 111, 17373–17378.

Guo, L., Hu, Y.J., Hu, Q.Q., Lin, J., Chen, J.M., Li, L.N., Fu, H.B., 2014b. Characteristics and chemical compositions of particulate matter collected at the selected metro stations of Shanghai, China. Sci. Total Environ. 496, 443–452.

Harris, S.J., Maricq, M.M., 2001. Signature size distributions for diesel and gasoline engine exhaust particulate matter. J. Aerosol Sci. 32, 749–764.

Harrison, R.M., Jones, A.M., Lawrence, R.G., 2003. A pragmatic mass closure model for airborne particulate matter at urban background and roadside sites. Atmos. Environ. 37, 4927–4933.

Hays, G.C., Richardson, A.J., Robinson, C., 2005. Climate change and marine plankton. Trends Ecol. Evol. 20, 337–344.

Hjortenkrans, D.S.T., Bergbäck, B.G., Häggerud, A.V., 2007. Metal emissions from brake linings and tires: case studies of Stockholm, Sweden 1995/1998 and 2005. Environ. Sci. Technol. 41, 5224–5230.

Ho, K., Lee, S., Guo, H., Tsai, W., 2004. Seasonal and diurnal variation of volatile organic compounds (VOCs) in the atmosphere of Hong Kong. Sci. Total Environ. 322, 155–166.

Ho, K.F., Lee, S.C., Ho, W.K., Blake, D.R., Cheng, Y., Li, Y.S., 2009. Vehicular emission of volatile organic compounds (VOCs) from a tunnel study in Hong Kong. 9 pp. 7491–7504.

Hu, Y.J., Lin, J., Zhang, S.Q., Kong, L.D., Fu, H.B., Chen, J.M., 2015. Identification of the typical metal particles among haze, fog, and clear episodes in the Beijing atmosphere. Sci. Total Environ. 511, 369–380.

Hu, Q.Q., Fu, H.B., Wang, Z.Z., Kong, L.D., Chen, M.D., Chen, J.M., 2016. The variation of characteristics of individual particles during the haze evolution in the urban Shanghai atmosphere. Atmos. Res. 181, 95–105.

Jacobson, 2001. Strong radiative heating due to the mixing state of black carbon in atmospheric aerosols. Nature 409, 695–697.

Kaegi, 2004. Chemical and morphological analysis of airborne particles at a tunnel construction site. J. Aerosol Sci. 35, 621–632.

Kang, S.N., Huang, H., Park, Y.M., Kim, H.K., Ro, C.U., 2008. Chemical compositions of subway particles in Seoul, Korea determined by a quantitative single particle analysis. Environ. Sci. Technol. 42, 9051–9057.

Kodavanti, U.P., Hauser, R., Christiani, D.C., Meng, Z.H., McGee, J., Ledbetter, A., 1998. Pulmonary responses to oil Al–Si particles in the rat differ by virtue of their specific soluble metals. Toxicol. Sci. 43, 204–212.

Kristensson, A., Johansson, C., Westerholm, R., Swietlicki, E., Gidhagen, L., Wideqvist, U., 2004. Real-world traffic emission factors of gases and particles measured in a road tunnel in Stockholm, Sweden. Atmos. Environ. 38, 657–673.

Laschober, C., Limbeck, A., Rendl, J., Puxbaum, H., 2004. Particulate emissions from on-road vehicles in the Kaisermühlen-tunnel (Vienna, Austria). Atmos. Environ. 38, 2187–2195.

Lee, S.C., Chiu, M.Y., Ho, K.F., Zou, S.C., Wang, X.M., 2002. Volatile organic compounds (VOCs) in urban atmosphere of HongKong. Chemosphere 48, 375–382.

Lerner, J.E., Sanchez, E.Y., Sambeth, J.E., Porta, A.A., 2012. Characterization and health risk assessment of VOCs in occupational environments in Buenos Aires, Argentina. Atmos. Environ. 55, 440–447.

Li, W.J., Shao, L.Y., Shi, Z.B., Li, J.J., Yang, S.S., 2008. Physical and chemical characteristics of individual mineral particles in an urban fog episode. China Environ. Sci. 29, 253–258.

Li, W.J., Shao, L.Y., Zhang, D.Z., Ro, C.U., Hu, M., Bi, X.H., Geng, H., Matsuki, A., Niu, H.Y., Chen, J.M., 2016. A review of single aerosol particle studies in the atmosphere of East Asia: morphology, mixing state, source, and heterogeneous reactions. J. Clean. Prod. 112, 1330–1349.

Lin, C.C., Chen, S.J., Huang, K.L., Hwang, W.I., Chang-Chien, G.P., Lin, W.Y., 2005. Characteristics of metals in nano/ultrafine/fine/coarse particles collected beside a heavily trafficked road. Environ. Sci. Technol. 39, 8113–8122.

Liu, C., Huang, X.F., Lan, Z.J., He, L.Y., 2012. A tunnel test for $PM_{2.5}$ emission factors ofmotor vehicles in Shenzhen. Environ. Sci. Technol. 12, 150–153.

Liu, Y.J., Zhang, T.T., Liu, Q.Y., Zhang, R.J., Sun, Z.Q., Zhang, M.G., 2014. Seasonal variation of physical and chemical properties in TSP, PM_{10} and $PM_{2.5}$ at a roadside site in Beijing and their influence on atmospheric visibility. Aerosol Air Qual. Res. 14, 954–969.

Liu, W.T., Ma, C.M., Liu, I.J., Han, B.C., Chuang, H.C., Chuang, K.J., 2015. Effects of commuting mode on air pollution exposure and cardiovascular health among young adults in Taipei, Taiwan. Int. J. Hyg. Environ. Health 218, 319–323.

Lowenthal, D.H., Zielinska, B., Chow, J.C., Watson, J.G., Gautam, M., Ferguson, D.H., 1994. Characterization of heavy-duty diesel vehicle emissions. Atmos. Environ. 28, 731–743.

Ma, C.M., Hong, G.B., Chang, C.T., 2011. Influence of traffic flow patterns on air quality inside the longest tunnel in Asia. Aerosol Air Qual. Res. 11, 44–50.

Mao, T., Wang, Y.S., Xu, H.H., Jiang, J., Wu, F.K., Xu, X.B., 2009. A study of the atmospheric VOCs of Mount Tai in June 2006. Atmos. Environ. 43, 2503–2508.

Meng, Z., Seinfeld, J.H., 1994. On the source of the submicrometer droplet mode of urban and regional aerosols. Aerosol Sci. Technol. 20, 253–265.

Na, K., Kim, Y.P., 2001. Seasonal characteristics of ambient volatile organic compounds in Seoul, Korea. Atmos. Environ. 35, 2603–2614.

Na, K., Kim, Y.P., Moon, K.C., 2003. Diurnal characteristics of volatile organic compounds in the Seoul atmosphere. Atmos. Environ. 37, 733–742.

Na, K., Moon, K.C., Kim, Y.P., 2005. Source contribution to aromatic VOC concentration and ozone formation potential in the atmosphere of Seoul. Atmos. Environ. 39, 5517–5524.

Na, K., Biswas, S., Robertson, W., Sahay, K., Okamoto, R., Mitchell, A., 2015. Impact of biodiesel and renewable diesel on emissions of regulated pollutants and greenhouse gases on a 2000 heavy duty diesel truck. Atmos. Environ. 107, 307–314.

Pio, C., Mirante, F., Oliveira, C., Matos, M., Caseiro, A., Oliveira, C., 2013. Size-segregated chemical composition of aerosol emissions in an urban road tunnel in Portugal. Atmos. Environ. 71, 15–25.

Pirjola, L., Parviainen, H., Hussein, T., Valli, A., Hameri, K., 2004. Atmos. Environ. 38, 3625–3635.

Querol, X., Pey, J., Minguillón, M.C., Pérez, N., Alastuey, A., Viana, M., 2008. PM speciation and sources in Mexico during the MILAGRO-2006 Campaign. Atmos. Chem. Phys. 8, 111–128.

Ristovski, Z.D., Morawska, L., Bofinger, N.D., Hitchins, J., 1998. Submicrom-eter and supermicrometer particulate emission from spark ignition vehicles. Environ. Sci. Technol. 32, 3845–3852.

Schmid, H., Pucher, E., Ellinger, R., Biebl, P., Puxbaum, H., 1997. Decadal reductions of tra$c emissions on a transit route in Austria-results of the Tauerntunnel experiment. Atmos. Environ. 35, 3585–3593.

Tong, Y.Q., Yin, Y., Qian, L., An, J.L., 2007. Analysis of the characteristics of hazy phenomena in Nanjing area. China Environ. Sci. 27, 584–588.

Wehner, B., Wiedensohler, A., 2003. Long term measurements of submicrometer urban aerosols: statistical analysis for correlations with meteorological conditions and trace gases. Atmos. Chem. Phys. 3, 867–879.

Woo, K.S., Chen, D.R., Chen, D.Y., Pui, Y.H., McMurry, P.H., 2001. Measurement of atlanta aerosol size distributions: observations of ultrane particle events. Aerosol Sci. Technol. 34, 75–87.

Zhang, S.J., Wu, Y., Zhao, B., Wu, X.M., Shu, J.W., Hao, J.M., 2017. City-specific vehicle emission control strategies to achieve stringent emission reduction targets in China's Yangtze River Delta region. J. Environ. Sci. 51, 75–87.

Zhou, R., Wang, S.S., Shi, C.Z., Wang, W.X., Zhao, H., Liu, R., 2014. Study on the traffic air pollution inside and outside a road tunnel in Shanghai, China. PLoS One 9, e112195.